Pergamon

NanoStructured Materials, Vol. 9, pp. 53-61, 1997
Elsevier Science Ltd

0965-9773/97 $17.00 + .00

PII S0965-9773(97)00018-4

INFLUENCES OF BINDING TRANSITIONS ON THE HOMOGENEOUS NUCLEATION OF MERCURY

R. B. McClurg[†], R. C. Flagan[†], and W. A. Goddard, III[‡,*]
[†]Spalding Laboratory (210-41)
[‡]Materials and Process Simulation Center, Beckman Institute (139-74)
Division of Chemistry and Chemical Engineering
California Institute of Technology, Pasadena, California 91125

Abstract – *Nucleation rates from supersaturated vapor are calculated for mercury. Previous measurements of nucleation rates using an upward thermal diffusion chamber demonstrated that critical supersaturations for Hg vapor are roughly three orders of magnitude lower than the predictions of the classical Becker-Doring-Zeldovich theory. [J. Martens, H. Uchtmann, and F. Hensel, J. Phys. Chem. 91, 2489 (1987)] This discrepancy was attributed to a metal-nonmetal transition in Hg clusters that occurs near the critical cluster size. [H. Uchtmann, K. Rademann, and F. Hensel, Annalen der Physik. 48, 207 (1991)] That view is supported by the similarity of cohesive energies and optical spectra for Hg clusters and rare gas clusters. [H. Haberland et al., Z. Phys. D 26, 8 (1993)] Using this analogy and the framework of the classical theory, we calculate nucleation rates that agree with the experiments within experimental uncertainties without any adjustable parameters. © 1997 Acta Metallurgica Inc.*

I. INTRODUCTION

Syntheses of nanostructured materials often involve spontaneous nucleation from a supersaturated phase followed by growth, agglomeration, coarsening, and/or ripening. The relative rates of these processes determine the product morphology and size distribution. Since unique properties of nanostructured materials derive from their structure, quantitative predictions of the kinetics of these processes are essential for a design and understanding of processing/structure/property/performance relations. In this paper, we illustrate the application of simple models to make quantitative rate predictions.

Although mercury is not a standard in nanomaterials circles, it will serve to illustrate our techniques and there is a wealth of literature describing its properties. Small mercury clusters ($n \leq 13$) are largely bound by van der Waals interactions while larger clusters ($n > 13$) are dominated by covalent interactions.(1–4) Evidence for this transition comes from photoionization, (1) 5d → 6p auto-ionizing spectroscopy, (2) and electron-

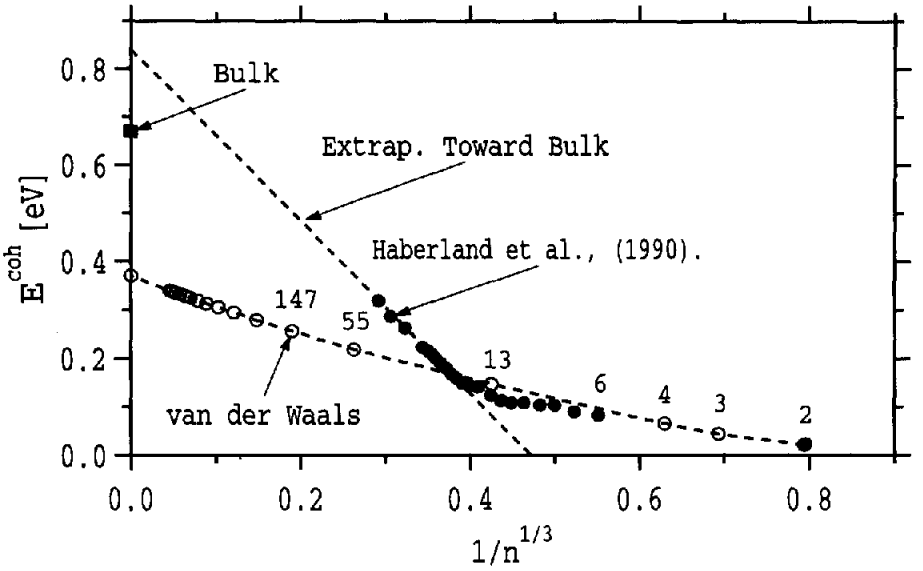

FIG. 1: Cohesive energy E^{coh} versus cluster size n plot showing the discontinuous first derivative near $n = 13$.

impact ionization. (3) Bennemann *et al.* (4) published a theory for this bond character transition that agrees well with experimental cohesive energies up to $n = 19$. The cohesive energy is the potential energy of the cluster at 0K. It is a large contributor to the cluster free energy up to the boiling point. At $n = 13$, their theory predicts a discontinuous first derivative of cohesive energy versus cluster size. Experimental values demonstrating that discontinuity are reproduced in Fig. 1. In this paper, we explore the implications of this discontinuity on the rate of nucleation of a condensed phase from a supersaturated vapor.

We will treat clusters on each side of this transition as if they were different "phases." Then we can write the free energy of each phase as an expansion about its bulk properties. We will truncate the series after three terms. (5)

$$G_n = n\mu_p + A_n\sigma_p\left(1 - \frac{2\delta_p}{r_n} + O(r_n^{-2})\right) \qquad [1]$$

$$p = \begin{cases} \text{vdW} & \text{for n} \leq 13 \\ \text{covalent} & \text{for n} > 13 \\ \text{metallic} & \text{for n} \to \infty \end{cases}$$

Thus, the chemical potential μ_p, surface tension σ_p, and Tolman length δ_p are (piecewise continuous) functions of the number of atoms in the cluster n or equivalently, the radius of the cluster r_n. This differential approach allows for a size-dependent "bulk" chemical

potential unlike the typical analysis which lumps all of the size dependence in the surface energy terms. (6)

The outline of the balance of our paper is as follows. We review the classical theory of nucleation in Section **II**. In Section **III**, we use that framework to show that, over a broad range of conditions, the rate-limiting step in nucleation is the formation of 13 atom clusters. The available experimental data is consistent with this interpretation. In Section **V**, we make quantitative predictions based on the classical nucleation theory and a simple model for Hg cluster properties, which is detailed in Section **IV**. The agreement with experimental results is excellent.

II. CLASSICAL NUCLEATION THEORY

According to classical theory, (7, 8) the flux (J_n) of clusters through a size (n) is

$$J_n = \alpha_n \beta A_n C_n - E_{n+1} C_{n+1} \qquad [2]$$

where α_n is the accommodation coefficient (commonly assumed to be unity), β is the flux of monomers through a unit area, A_n is the surface area of the cluster, C_n is the number concentration, and E_n is the frequency of monomer evaporation from an n-mer. To determine E_n, we follow the approach of Katz.(8) Applying detailed balancing at full thermodynamic equilibrium yields

$$J_n^{eq} = 0 = \alpha_n \beta^{eq} A_n C_n^{eq} - E_{n+1}^{eq} C_{n+1}^{eq}. \qquad [3]$$

Assuming that the evaporation rate is independent of the saturation ratio, i.e. $E_{n+1} = E_{n+1}^{eq}$, leads to the following estimate for E_{n+1}.

$$E_{n+1} = \alpha_n \beta^{eq} A_n C_n^{eq} / C_{n+1}^{eq} \qquad [4]$$

Substituting Eq. (4) into Eq. (2),

$$J_n = \alpha_n \beta A_n C_n^{eq} \left[\frac{C_n}{C_n^{eq}} - \frac{\beta^{eq} C_{n+1}}{\beta C_{n+1}^{eq}} \right] \qquad [5]$$

multiplying and dividing by $(\beta^{eq}/\beta)^n$, and rearranging gives

$$\frac{J_n}{\alpha_n \beta A_n C_n^{eq} (\beta/\beta^{eq})^n} = \frac{C_n}{C_n^{eq}} \left(\frac{\beta^{eq}}{\beta} \right)^n - \frac{C_{n+1}}{C_{n+1}^{eq}} \left(\frac{\beta^{eq}}{\beta} \right)^{n+1}. \qquad [6]$$

For steady state nucleation, $J_1 = J_2 = ... = J_b = J$. Summing Eq. (6) over n yields

$$J \sum_{n=1}^{b} \frac{1}{\alpha_n \beta A_n C_n^{eq} (\beta/\beta^{eq})^n} = \frac{C_1}{C_1^{eq}} \left(\frac{\beta^{eq}}{\beta} \right) - \frac{C_{b+1}}{C_{b+1}^{eq}} \left(\frac{\beta^{eq}}{\beta} \right)^{b+1}. \qquad [7]$$

From the kinetic theory of gases,

$$\beta = P/(2\pi m k T)^{1/2} \qquad [8]$$

$$\beta/\beta^{eq} = P/P^{vap} = C_1/C_1^{eq} = S \quad [9]$$

where P is the monomer pressure and S is the saturation ratio. By the law of mass action

$$C_n^{eq} = C_1^{eq} \exp(-\Delta G_n/kT) \quad [10]$$

$$\Delta G_n = G_n - n\mu_{bulk} \quad [11]$$

where G_n is the free energy of a cluster of n atoms and μ_{bulk} is the bulk chemical potential for the equilibrium phase of the bulk material, i.e. metallic mercury. Finally, using Eqs. (9) and (10) and allowing b to become large gives the desired form for the nucleation rate.

$$J = \beta / \sum_{n=1}^{\infty} \left[\alpha_n A_n C_1^{eq} \exp\left(n \ln S - \frac{\Delta G_n}{kT} \right) \right]^{-1} \quad [12]$$

III. CRITICAL SIZE DETERMINATION

Substituting Eqs. (11) into Eq. (12) gives the nucleation rate (J) in terms of the cluster free energy (G_n).

$$J = \beta C_1^{eq} / \sum_{n=1}^{\infty} \left[\alpha_n A_n \exp\left(n \ln S + \frac{(n\mu_{bulk} - G_n)}{kT} \right) \right]^{-1} \quad [13]$$

Since the product $(\alpha_n A_n)$ changes slowly with n, the relative magnitude of each term of the summation is determined largely by the argument of the exponential. The value of n that minimizes the argument is called the critical cluster size (n^*). Because G_n is not a smooth function of n, some care must be taken in determining n^*. For sufficiently low(high) saturation ratios, the critical cluster size will be larger(smaller) than 13 atoms and one can differentiate the argument with respect to n to find the critical size. For a range of intermediate saturation ratios, the argument is minimized at the kink in G_n at $n = 13$. This is shown graphically in Fig. 2.

We define $S_l(S_h)$ as the lower(higher) saturation ratio such that the critical cluster size is 13 atoms. The size of the window defined by S_h/S_l can be estimated assuming that the other contributions to the free energy are smooth at $n = 13$.

$$S_h/S_l \approx \exp\left[\frac{-\left(dE^{coh}/dn\right)_{13^-} + \left(dE^{coh}/dn\right)_{13^+}}{kT} \right] \quad [14]$$

Fitting functions to the cohesive energy leads to

$$S_h/S_l \approx \exp\left(963K/T\right) \quad [15]$$

Therefore, at room temperature we expect a critical size of 13 atoms over a factor of 25 in saturation ratios. According to the nucleation theorem, (10, 11) the nucleation rate is of the form

$$J = J_0 S^{(n^*+1)} \quad [16]$$

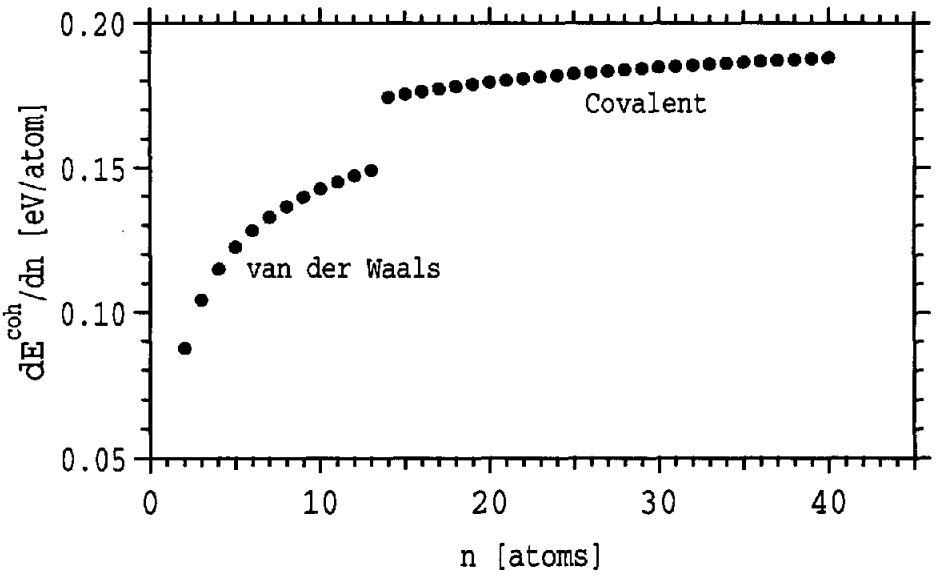

FIG. 2: For a wide range of S, the critical size is 13 atoms due to the kink in E^{coh} (and G_n) at that size.

Therefore, on a log-log plot, loci of nucleation rates (at a given temperature) as a function of the saturation ratio (S) should fall on a straight line of slope 14 over this range of S values. This is qualitatively consistent with experimental data. (12) We will make the comparison quantitative in the following sections.

IV. NUCLEATION RATE CALCULATION

Since clusters in the covalent size range ($n > 13$) are much more strongly bound than in the van der Waals size range ($n \leq 13$), the terms in the summation of Eq. (13) after the 13th contribute negligibly to the sum for sufficiently large S values. We will truncate the sum after the 13th term. For the conditions discussed below, we estimate that this introduces an error of less than 1%. For ideal monatomic gas vapors, the chemical potential can be related to the vapor pressure as follows. (13)

$$\mu/kT = \ln\left(\frac{P^{vap}h^3}{(2\pi m)^{3/2}(kT)^{5/2}}\right) \qquad [17]$$

Using this result in Eq. (13) gives

$$J = \beta C_1^{eq} / \sum_{n=1}^{13}\left[\alpha_n A_n S^n \left(\frac{P_{bulk}^{vap}}{P_{vdW}^{vap}}\right)^n \exp\left(\frac{-A_n\sigma_{vdW}}{kT}(1 - 2\delta_{vdW}/r_n)\right)\right]^{-1} \qquad [18]$$

where β and C_1^{eq} are vapor properties, P_{vdW}^{vap}, σ_{vdW}, and δ_{vdW} are the bulk properties that mercury would have if it remained a van der Waals fluid up to bulk sizes, and P_{bulk}^{vap} is the vapor pressure of bulk (metallic) mercury. Next, we summarize our estimates of these material properties.

Vapor Properties

We will treat the vapor as an ideal gas. Then the equilibrium monomer concentration (C_1^{eq}) and the monomer flux (β) can be calculated from the ideal gas law and the kinetic theory of gases.

$$C_1^{eq} = P^{vap}/kT \quad [19]$$

$$\beta = P/(2\pi mkT)^{1/2} = SP^{vap}/(2\pi mkT)^{1/2} \quad [20]$$

van der Waals Properties

To model the vdW phase of Hg, we have used an effective Lennard-Jones potential.

$$\begin{aligned} \epsilon &= \rho^{-12} - 2\rho^{-6} \quad [21] \\ \epsilon &= E/D_e \\ \rho &= r/R_e \end{aligned}$$

Here E is the pairwise interaction energy and r is the distance between pairs of atoms in clusters of up to 13 atoms. The most recent experimental determination and *ab initio* calculation of the equilibrium distance for the dimer are 3.63 and 3.73Å, respectively. (14, 15) Similarly, the dimer cohesive energy has been estimated at 0.043 and 0.047eV by experiment and theory. (16, 15) The energy parameter D_e is larger than the cohesive energy due to the zero-point energy.

$$D_e = E^{coh} + \omega\hbar/2 \quad [22]$$

Here, ω is the dimer vibrational frequency which is approximately 19cm^{-1} for mercury.(14–16) To be consistent, we use the calculated values.

$$\begin{aligned} R_e &= 3.73\mathring{A} \pm 3\% \quad [23] \\ D_e &= 0.047eV \pm 3\% \\ m &= 200.59amu \end{aligned}$$

We use correlations from the literature to estimate P_{vdW}^{vap}, σ_{vdW}, and δ_{vdW} given the Lennard-Jones potential. (17–19) In addition, we estimate the sublimation pressure using the Classius-Clapeyron equation, and we assume that the solid surface tension is constant at its triple point value.

Metallic Properties

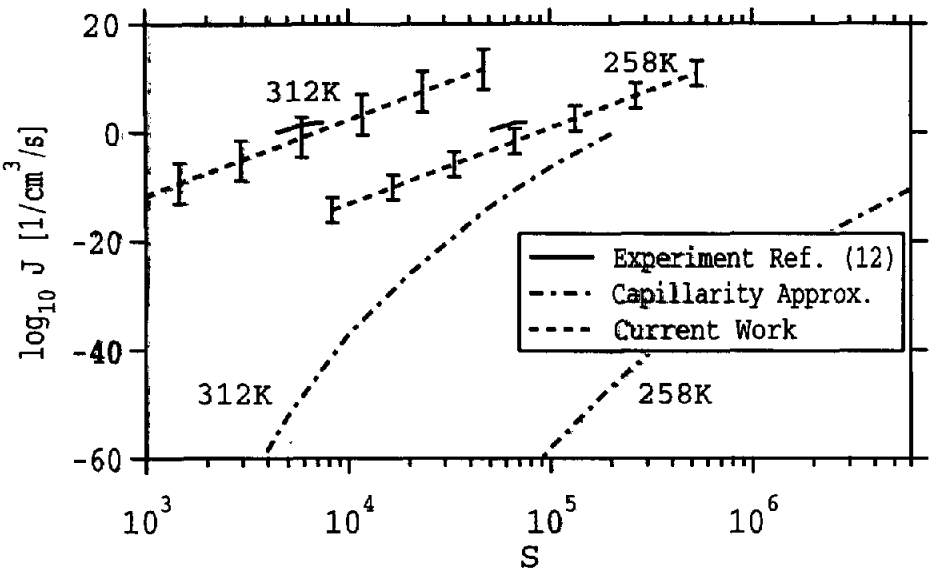

FIG. 3: Nucleation rates (J) as a function of saturation ratio (S).

The only metallic Hg property that appears in Eq. 18 is the bulk vapor pressure. We should point out that this can be eliminated since

$$S^n \left(\frac{P_{bulk}^{vap}}{P_{vdW}^{vap}} \right)^n = \left(\frac{P_{Hg}}{P_{vdW}^{vap}} \right)^n . \qquad [24]$$

This is consistent with our assumption that the nucleation event involves only non-metallic mercury clusters. Although this relation can be used to simplify the nucleation rate calculation, we have chosen to leave Eq. 18 in its present form to emphasize the influence of the binding character transition and to facilitate comparisons with other calculations of nucleation rate (J) as a function of saturation ratio (S). DeKruif, VanGinkel, and Langenberg (20) critically reviewed the low temperature vapor pressure data for Hg and present a correlation that agrees within 3% from the triple point (234K) to at least 1050K. (21) We will also make use of a correlation of the bulk surface tension. (22)

V. RESULTS AND DISCUSSION

In Fig. 3, we show experimental measurements of mercury vapor nucleation rates and two estimates of that rate. The estimate from the current work is within the error bars (imposed primarily by the uncertainty in the Lennard-Jones energy parameter). (D_e) The other estimate is based on the capillarity approximation. In the capillarity approximation, the free energy difference (ΔG) is estimated using Eq. 2 and the bulk chemical potential and surface energy. The asymptotic expansion about the bulk equi-

librium phase is truncated after the second term. For further discussion, see Refs. (7,8). The capillarity approximation leads to large errors due to the metal/nonmetal transition that occurs around 13 mercury atoms. This is the hallmark of nanoscale materials: they have properties unlike single atoms or bulk.

The simple model that we have used to estimate the nucleation rate for mercury suggests that other systems are tractable, but that the unique character of nanoscale clusters must be incorporated in those estimates. Simple methods based on bulk properties are likely to give wildly erroneous results.

We are currently refining our model using *ab initio* calculations to obtain effective Lennard-Jones parameters appropriate for the 13-mer. (23)

VI. ACKNOWLEDGMENTS

Partial support of this work was provided by grants from NSF (CHE 95-22179) and from the International Fine Particle Research Institute.

---

1. K. Rademann, B. Kaiser, U. Even, and F. Hensel, Phys. Rev. Lett. 59, 2319 (1987).
2. C. Bréchignac, M. Broyer, Ph. Cahuzac, G. Delacretaz, P. Labastie, J. P. Wolf, and L. Wöste, Phys. Rev. Lett. 60, 275 (1988).
3. H. Haberland, H. Kornmeier, H. Langosch, M. Oschwald, and G. Tanner, J. Chem. Soc. Faraday Trans. 86, 2473 (1990).
4. M. E. Garcia, G. M. Pastor, and K. H. Bennemann, Phys. Rev. Lett. 67, 1142 (1991).
5. R. C. Tolman, J. Chem. Phys. 17, 333 (1949).
6. R. B. McClurg, R. C. Flagan, and W. A. Goddard, J. Chem. Phys. 102, 3322 (1995).
7. D. W. Oxtoby, J. Phys. Condens. Matter. 4, 7627 (1992).
8. J. L. Katz, Pure Appl. Chem. 64, 1661 (1992).
9. R. R. Hultgren, *Selected values of the thermodynamic properties of the elements*, p.236, Am. Soc. for Metals, Metals Park, Ohio (1973).
10. D. Kashchiev, J. Chem. Phys. 76, 5098 (1982).
11. D. W. Oxtoby and D. Kashchiev, J. Chem. Phys. 100, 7665 (1994).
12. J. Martens, H. Uchtmann, and F. Hensel, J. Phys. Chem. 91, 2489 (1987).
13. T. L. Hill, *Statistical Thermodynamics*, p.104, Dover, New York (1986).
14. R. D. van Zee, S. C. Blankespoor, and T. S. Zwier, J. Chem. Phys. 88, 4650 (1988).
15. M. Dolg and H. J. Flad, J. Phys. Chem. 100, 6147 (1996).

16. A. Zehnacker, M. C. Duval, C. Jouvet, C. Lardeux-Dedonder, D. Solgadi, B. Soep, and O. J. Benoist d'Azy, J. Chem. Phys. 86, 6565 (1987).

17. A. Lotfi, J. Vrabec, and J. Fischer, Mol. Phys. 76, 1319 (1992).

18. J. E. Hunter and W. P. Reinhardt, J. Chem. Phys. 103, 8627 (1995).

19. The Tolman length is nearly independent of temperature for $T/T_c \leq 0.80$. [R. B. McClurg, R. C. Flagan, and W. A. Goddard, submitted to J. Chem. Phys.] For our system, this requires $kT/D_e \leq 1.06$ or $T < 575K$.

20. C. G. DeKruif, C. H. D. VanGinkel, and A. Langenberg, Recueil. 92, 599 (1973).

21. R. H. Perry and D. W. Green (eds.), *Perry's Chemical Engineers' Handbook* 6th ed.,p.3-201, McGraw-Hill, New York (1984). We suspect that the equilibrium pressure at 333.15K in the table has transposed digits and should read $3.536 \cdot 10^{-5}$bar.

22. J. J. Jasper, J. Phys. Chem. Ref. Data 1, 841 (1972).

23. R. B. McClurg, B.-L. Tsai, R. C. Flagan, and W. A. Goddard, work in progress.